



Design and Experimental Research of Cable-Driven Upper-Limb Rehabilitation Robot

Xiangshu Wu, Yupeng Zou^(✉), Qiang Zhang, Baolong Zhang, Xuebin Gu,
and Jiping Zhang

China University of Petroleum, Qingdao 266580, China
zouyupeng@upc.edu.cn

Abstract. To help patients with upper-limb dysfunction in rehabilitation training, a parallel cable-driven upper-limb rehabilitation robot was proposed. The robot has advantages in modular design, simple mechanism, low cost, lightweight and good human-machine compatibility. The robot can help patients with upper-limb dysfunction to carry out various forms of rehabilitation training. Trajectory planning, kinematics analysis, workspace verification and human-machine experimental research were also carried out for shoulder joint flexion/extension. The results show that the parallel flexible cable-driven upper-limb rehabilitation robot in this paper has certain significance for patients to carry out rehabilitation training.

Keywords: Upper-limb rehabilitation · Cable-driven · Kinematics analysis · Human-machine experiment

1 Introduction

As the global aging of the population is becoming increasingly serious, stroke has become the second leading cause of death in people over 60 years old [1]. In addition, the number of patients with upper-limb dysfunction caused by natural disasters, emergencies and other acquired causes is also increasing. How to maximize the recovery of normal motor ability of patients with upper-limb dysfunction is a difficult problem in the field of rehabilitation medicine. Compared with the artificial rehabilitation, the upper-limb rehabilitation robot has the advantages in precise rehabilitation training, low cost and high efficiency. Therefore, it has unique advantages to realize the functional recovery of the affected limb through the upper-limb rehabilitation robot [2].

According to the different structure forms, upper-limb rehabilitation robot can be divided into two types: the exoskeleton rehabilitation robot and the end traction rehabilitation robot [3]. The exoskeleton upper-limb rehabilitation robot realizes rehabilitation training by controlling the exoskeleton to drive the coordinated movement of the affected limb. The Chicago Institute of Rehabilitation and the University of California had jointly developed a 3-DOF upper-limb rehabilitation robot ARM Guide. The robot has an active degree of freedom, the linear guide is driven by the motor to realize the flexion/extension

movement of the upper-limb [4, 5]. A 5-DOF SAIL upper-limb rehabilitation robot was designed by the University of Southampton in the United Kingdom. The torsion spring elastic auxiliary support mechanism was installed at the shoulder and elbow joints. VR technology was combined with electrical signal stimulation of upper-limb muscles. The robot realizes upper-limb rehabilitation through the above measures [6]. The main mechanism of the end traction upper-limb rehabilitation robot is an ordinary linkage mechanism or a tandem robot mechanism. Through the mechanism at the end of the robot to pull the affected limb to complete the rehabilitation. Hogan proposed a robot system with gravity compensation—the 2-DOF arm planar rehabilitation robot system MIT-MANUS [7]. Subsequently, a 2-DOF wrist rehabilitation robot was also proposed [8, 9]. The two rehabilitation robots formed a complete upper-limb 4-DOF rehabilitation system. The GENTLE/S upper-limb rehabilitation robot developed by the University of Reading used cable to reduce the weight of the affected limb. Based on the drive of Haptic MASTER industrial robot, the shoulder and elbow joint were trained [10, 11]. Many institutions have conducted in-depth research on upper-limb rehabilitation robot. However, the research on the size, structure, human-machine compatibility and secondary injury prevention of the upper-limb rehabilitation robot can still be carried out in-depth [12].

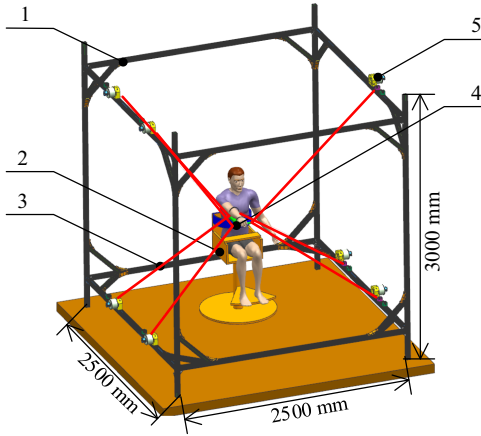
The cable-driven robot is a new type of robot. It uses cable to replace traditional rigid connectors. By controlling the motor to drive the pulley to change the length of cable, the pose control of the end effector is completed. British Jensen designed a 9-cable drive parallel robot SACSO. The literature detailed the kinematics, cable tension and dynamic characteristics of the object under the redundant constraint state driven by 9 cables. The wind tunnel model test was carried out [13]. Williams of Ohio State University designed a simulation dynamics and control system of the planar translational cable-oriented robot (CDDR). It improved the cable interference problem of the existing CDDRs, and avoided applying negative cable tension to the environment during dynamic movement [14]. The cable-driven robot has the advantages in large workspace, high inertia ratio, fast response of load speed, and easy reorganization of robot mechanism [15, 16].

To solve the problems of the upper-limb rehabilitation robot mentioned above, a cable-driven upper-limb rehabilitation robot (CULR) with features of modular design, simple structure, and good human-machine compatibility was presented in this paper. Through the shoulder flexion/extension, trajectory planning, kinematics analysis, workspace verification and human-machine experiment research were carried out. Based on these, the robot assisted patients in different rehabilitation stages to develop a variety of task-oriented rehabilitation.

2 Cable-Driven Upper-Limb Rehabilitation Robot

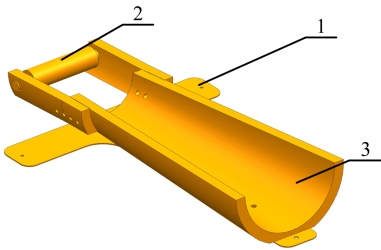
2.1 Composition of CULR

As shown in Fig. 1, CULR is composed of frame, seven groups of cable-driven units, rotating seat, cable and movable platform. Movable platform is shown in Fig. 2. By controlling the angle change of the rollers in the seven groups of cable-drive units, the structure of the cable-drive units is shown in Fig. 3, the coordinated variation of the seven cables are realized. Therefore, the platform can be pulled to drive the affected limb



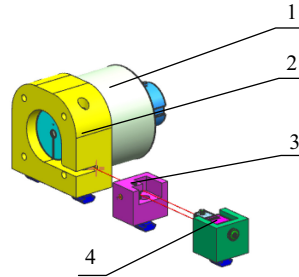
1. Frame; 2. Rotating seat; 3. Cable; 4. Movable platform; 5. Cable-driven unit.

Fig. 1. The composition of CULR.



1. Traction point; 2. Armrest; 3. Movable platform.

Fig. 2. The structure of movable platform



1. Permanent magnet DC torque motor; 2. Motor bracket 3. Guide wheel; 4. Tension sensor.

Fig. 3. The structure of the cable-drive unit

according to the planned trajectory to perform rehabilitation. The contact part between the patient and robot is small, and the human-machine compatibility is good.

2.2 Shoulder Flexion and Extension

This paper has planned a trajectory that simulated the flexion / extension movement of the shoulder joint in the xOz plane (as shown in Fig. 4). The law of forearm center of mass movement is as formula (1), where the shoulder joint rotation angle θ_s ranges from -30° to 30° (anti-clockwise rotation is positive, clockwise rotation is negative).

$$\begin{cases} x = -430(\cos(u) - 1) \\ z = 430 \sin(u) \\ \theta_y = u \end{cases} \quad (-\pi/6 \leq u \leq \pi/6) \quad (1)$$

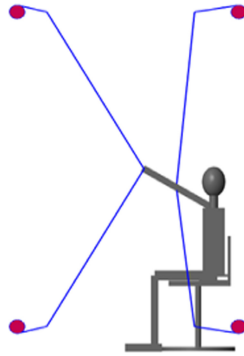


Fig. 4. Shoulder flexion and extension

3 Robot Kinematics Analysis

3.1 Inverse Kinematics

Figure 5 shows the 3R3T (three rotation and three translation) parallel cable-drive mechanism (PCDM). The seven driving points $M_i (X_{Mi}, Y_{Mi}) (i = 1, 2, \dots, 7)$ of mechanism are $M_1 (-a, -b, -e), M_2 (a, -b, -e), M_3 (a, b, -e), M_4 (-a, b, -e), M_5 (-a, -b, e), M_6 (a, b, e), M_7 (-a, b, e)$ (a, b and e are greater than 0), the global rectangular coordinate system $Oxyz$ is located at the center of the cube composed of seven driving points. The seven (three) traction points of the movable platform (some traction points coincide) are shown in Fig. 5. The seven cables $P_i M_i (i = 1, 2, \dots, 7)$ are connected to the seven (three) traction points of the movable platform by the output of seven driving points. The local coordinate system of the movable platform is $Px_p y_p z_p$, the pose of the center of movable platform in the global rectangular coordinate system is expressed as $P (x, y, z, \theta_x, \theta_y, \theta_z)$. $P_i (X_{Pi}, Y_{Pi}, Z_{Pi})$ represents the traction point in the local coordinate system, then

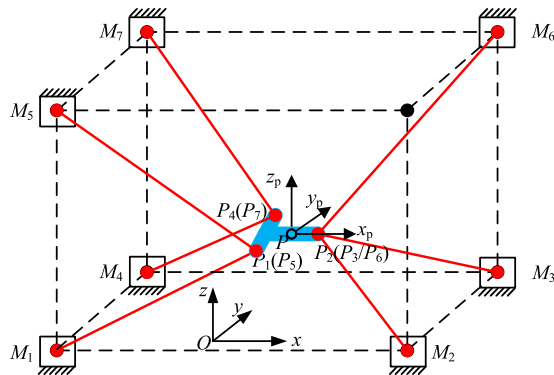


Fig. 5. Mechanism model of 3R3T PCDM

the point P_i ($i = 1, 2, \dots, 7$) in the global coordinate system can be expressed as:

$$\begin{bmatrix} x_{P_i} \\ y_{P_i} \\ z_{P_i} \end{bmatrix} = \begin{bmatrix} x \\ y \\ z \end{bmatrix} + \mathbf{D} \begin{bmatrix} X_{P_i} \\ Y_{P_i} \\ Z_{P_i} \end{bmatrix} \tag{2}$$

Among them, \mathbf{D} is the direction cosine vector.

$\mathbf{r}_i = \mathbf{P}P_i$ ($i = 1, 2, \dots, 7$) is the vector from the center point P of the movable platform to the traction point P_i . $\mathbf{L}_i = \mathbf{P}_iM_i$ is the vector from the traction point P_i to the driving point M_i , then the length of the cable can be expressed as $l_i = \|\mathbf{L}_i\|$. $\mathbf{u}_i = \mathbf{L}_i/l_i$ is the unit vector of the i th cable, t_i is the force value of the i th cable, then the tension vector of the i th cable acting on the movable platform is $\mathbf{t}_i = \mathbf{u}_i t_i$. According to the principle of robot mechanism and mathematics vector closure, the length of the cable is:

$$\mathbf{l} = [l_1 \ l_2 \ l_3 \ l_4 \ l_5 \ l_6 \ l_7]^T \tag{3}$$

3.2 Forward Kinematics

The variation of the cable has been calculated during the movement of the movable platform, the next step is to control the length of the cable in real time to pull the movable platform to complete the expected action. Because there is no root formula for solving the nonlinear equations of the cable length, so the approximate solution of cable length is solved by numerical calculation, that is, the Newton-Raphson iterative method is used to solve the Eq. (3). The principle of this method is to substitute the guessed solution, iterate layer by layer, and produce an ideal solution within the allowable error range after a finite iteration step. The specific solution process is as follows:

According to formula 3, construct the following formula:

$$F_i(\mathbf{X}) = \|\mathbf{L}_i\|^2 - l_i^2, \ i = 1, 2, \dots, 7 \tag{4}$$

$$\mathbf{J}_i = \left[\frac{\partial F_i}{\partial x} \ \frac{\partial F_i}{\partial y} \ \frac{\partial F_i}{\partial z} \ \frac{\partial F_i}{\partial \alpha} \ \frac{\partial F_i}{\partial \beta} \ \frac{\partial F_i}{\partial \gamma} \right]_{1 \times 6}, \ i = 1, 2, \dots, 7 \tag{5}$$

$$\mathbf{J} = [J_1 \ J_2 \ J_3 \ J_4 \ J_5 \ J_6 \ J_7]_{7 \times 6}^T, \ i = 1, 2, \dots, 7 \tag{6}$$

$$\mathbf{F}(\mathbf{X}) = [F_1(\mathbf{X}) \ F_2(\mathbf{X}) \ F_3(\mathbf{X}) \ F_4(\mathbf{X}) \ F_5(\mathbf{X}) \ F_6(\mathbf{X}) \ F_7(\mathbf{X})]^T \tag{7}$$

$$\mathbf{X} = [x \ y \ z \ \alpha \ \beta \ \gamma]^T \tag{8}$$

$$\mathbf{J} \delta \mathbf{X}_K = -\mathbf{F}(\mathbf{X}) \ \text{or} \ \delta \mathbf{X}_K = -\mathbf{J}^+ \mathbf{F}(\mathbf{X}) \tag{9}$$

$$\mathbf{X}_{K+1} = \mathbf{X}_K + \delta \mathbf{X}_K \tag{10}$$

$$\|\delta \mathbf{X}_K\| < \varepsilon \tag{11}$$

According to matrix theory, the pseudo-inverse of Newton-Raphson Jacobian matrix J is $J^+ = (J^T J)^{-1} J^T$.

Through the above method, the forward kinematics analysis is carried out on the 3R3T PCDM. The center pose of movable platform can be obtained according to the length of the cable for subsequent motion control.

3.3 Workspace Analysis

The 3R3T PCDM in this paper is a fully constrained mechanism. Considering the general situation, when solving the workspace of the 3R3T PCDM, the DOF of the mechanism is n . Assuming that the pose of the movable platform in the global Cartesian coordinate system is X^n , $T \in R^m (T \geq 0)$ is the tension of each cable, $F \in R^n$ is a force spiral vector acting on the movable platform. If $J^T T = F$ holds, X^n is the controllable workspace of the movable platform [17]. The tension matrix is $T = [t_1 \dots t_m]^T$, and the J^T is the structure matrix, $J^T = \begin{bmatrix} u_1 & \dots & u_m \\ r_1 \times u_1 & \dots & r_m \times u_m \end{bmatrix}$.

Figure 6 shows the n -DOF mechanism model of PCDM. Assuming that the force and torque acting on the movable platform by the cable are removed, f_p and τ_p are the external force and torque.

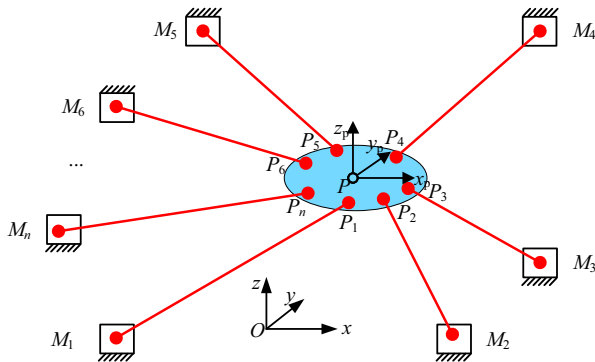


Fig. 6. n -DOF mechanism model of PCDM.

According to the D'Alembert principle, the force spiral balance equations of the movable platform are:

$$\sum_{i=1}^m t_i + f_p = 0 \tag{12}$$

$$\sum_{i=1}^m r_i \times t_i + \tau_p = 0 \tag{13}$$

According to (12) and (13),

$$J^T T = \begin{bmatrix} u_1 & \dots & u_m \\ r_1 \times u_1 & \dots & r_m \times u_m \end{bmatrix} T = F \tag{14}$$

In the formula, F is the external force spiral matrix acting on the movable platform, $F = [-f_p - \tau_p]^T$.

If the workspace has practical significance, the pose of movable platform of the PCDM must meet the following conditions:

- (a) The movable platform is controllable, that is $J^T T = F$;
- (b) The tension value of the cable is greater than 0, that is, $t_i > 0 (i = 1, 2, \dots, m)$, and it is within the allowable tension range;
- (c) There is no singular position in the movement of the movable platform, that is $\text{rank}(J^T) = n$;
- (d) The PCDM has sufficient strength.

In addition, based on the tension t_i of each cable must be greater than 0, that is $T = (I - J^{T+} J) > 0$ (J^{T+} is the pseudo-inverse matrix of the cable structure matrix J^T), Kawamura and Verhoeven obtained the necessary and sufficient condition for judging whether the movable platform pose X^n in the PCDM is in the controllable workspace: the zero space structure matrix J^T is greater than 0, which is $N(J^T) > 0$ [18].

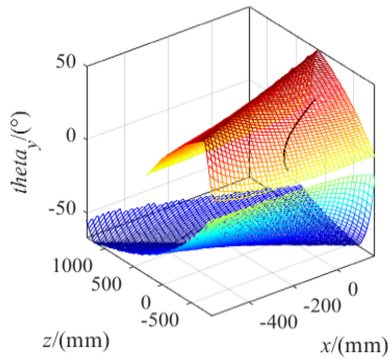


Fig. 7. Relationship between shoulder joint flexion/extension movement trajectory and workspace

Therefore, for the n -DOF PCDM, only $\text{rank}(J^T) = n$ and $N(J^T) > 0$ are satisfied at the same time, the pose of the movable platform is within the controllable workspace.

When the upper-limb is driven by the movable platform to conduct shoulder joint flexion/extension, the relationship between the motion trajectory of the center of mass of forearm and the workspace is shown in Fig. 7. It can be seen from the figure that the trajectory of the center of the movable platform (the center of mass of forearm) is completely enclosed in the robot’s workspace. Therefore, the 3R3T parallel CULR can meet the requirements of upper-limb basic rehabilitation. At this time the length changes of each cable under the two motion trajectories are shown in Fig. 8, it will pave the way for the subsequent experimental verification.

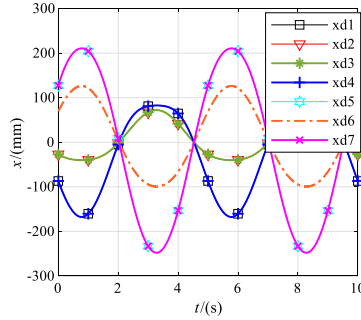


Fig. 8. Cable variation of shoulder joint flexion/extension movement

4 Experimental Research on CULR

This experimental research was carried out based on the LINKS real-time semi-physical simulation system. In the experiment, a healthy adult male with a height of 178 cm and a weight of 63 kg was selected as the experimental object. The robot drove the experimental object to move the upper-limb to simulate the shoulder flexion/extension. The movable platform drove the subject's upper-limb to make a circular motion with a rotation angle θ of 60° and a period T of 5 s. The experimental process is shown in Fig. 9, and the experimental results are shown in Fig. 10.

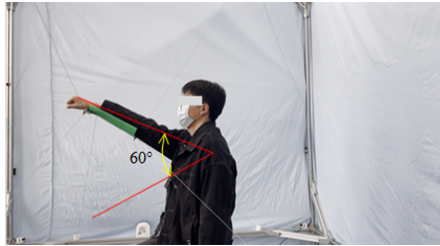
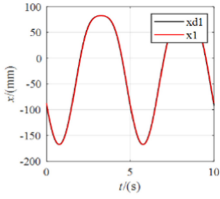
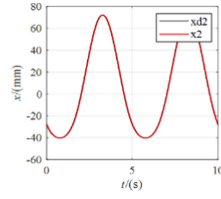


Fig. 9. Shoulder joint flexion/extension exercise experiment

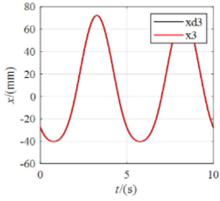
From the experimental results in Fig. 10(a) to 10(g), in the experimental research of shoulder joint flexion/extension rehabilitation exercise, the actual length change of the seven cables basically is coincide with the given amount. It can be seen from Fig. 10(h) that the maximum error of the cable length change amount is about 10 mm. The extremely small error is caused by the cable-drive unit mechanism itself. But the experimental effect reached the expected goal and met the requirements. It can be seen from Fig. 10(i) and 10(j) that the change range of tension and linear velocity of each cable is small, and in a controllable range, without large mutation. The effectiveness and safety of the upper-limb rehabilitation robot are verified.



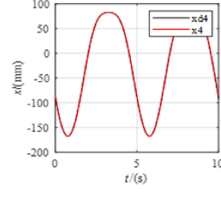
(a) Length changes of cable 1



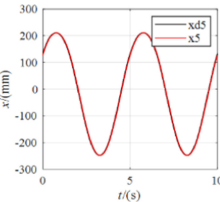
(b) Length changes of cable 2



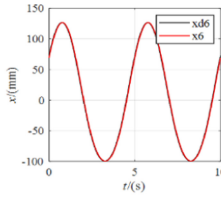
(c) Length changes of cable 3



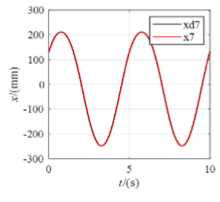
(d) Length changes of cable 4



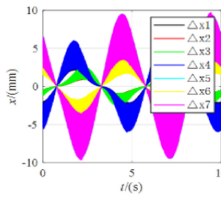
(e) Length changes of cable 5



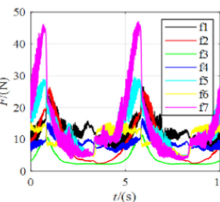
(f) Length changes of cable 6



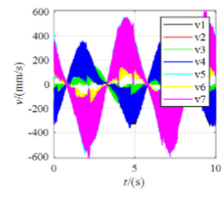
(g) Length changes of cable 7



(h) Error of each cable length change amount



(i) Tension of each cable



(j) Linear velocity of each cable

Fig. 10. Experimental curve of shoulder joint flexion/extension exercise

By analyzing the experimental results, the following conclusions can be drawn:

- (a) By analyzing the relationship between the actual length change of the flexible cable and the given amount, the effectiveness of the designed position servo controller isSS verified.
- (b) The human-machine experiment has completed the simulation of the flexion/extension movement of the shoulder joint, the experimental effect is good. The feasibility of the upper-limb rehabilitation robot is verified, and the rehabilitation has high efficiency and diversified forms.
- (c) By interviewing the subject's feelings and analyzing the feedback data during the experiment, the CULR drives the upper-limb for rehabilitation with less human-machine interference and high comfort.

5 Conclusion

In this paper, a cable-driven upper-limb rehabilitation robot was proposed based on 3R3T PCDM. The shoulder joint flexion/extension movement trajectory was planned, and the kinematics analysis of the 3R3T PCDM was carried out, the method of controllable workspace analysis was proposed, finally, the change law of cable was obtained. The human-machine experiment that simulated the rehabilitation of shoulder joint flexion/extension exercise has been completed and the experimental effect is good. This paper has laid a strong foundation for the research of parallel cable-driven upper-limb rehabilitation robot.

Based on this work, the kinematic characteristics will be analyzed further, and the control strategies of different rehabilitation modes will also be studied. The results were prepared for the following prototype experiment and human-machine experiment.

References

1. Jiang, X.Z.: Servo Control of Joint Driven by Two Pneumatic Muscles in Opposing Pair Configuration for Rehabilitation Robot. Huazhong University of Science and Technology, Wuhan (2011)
2. Yang, Q., Cao, D., Zhao, J.: Analysis on state of the art of upper limb rehabilitation robots. *Robot* **35**(5), 630–640 (2013)
3. Yang, Z., Zi, B., Chen, B.: Mechanism design and kinematic analysis of a waist and lower limbs cable-driven parallel rehabilitation robot. In: 2019 IEEE 3rd Advanced Information Management, Communicates, Electronic and Automation Control Conference (IMCEC), pp. 723–727 (2019)
4. Kahn, L.E., Zygmant, M.L., Rymer, W.Z., et al.: Robot-assisted reaching exercise promotes arm movement recovery in chronic hemiparetic stroke: a randomized controlled pilot study. *J. Neuro Eng. Rehab.* **3**(12), 1–13 (2006)
5. Reinkensmeyer, D.J., Kahn, L.E., Averbuch, M., et al.: Understanding and treating arm movement impairment after chronic brain injury: progress with the ARM guide. *J. Rehabil. Res. Dev.* **37**(6), 653–662 (2000)
6. Cai, Z., Tong, D., Meadmore, K.L., et al.: Design & control of a 3D stroke rehabilitation platform. In: IEEE International Conference on Rehabilitation Robotics. Piscataway. IEEE (2011)

7. Fasoli, S., Krebs, H., Stein, J., Frontera, W., Hogan, N.: Effects of robotic therapy on motor impairment and recovery in chronic stroke. *Arch. Phys. Med. Rehab.* **84**(4), 477–482 (2003)
8. Charles, S.K., Krebs, H.I., Volpe, B.T., et al.: Wrist rehabilitation following stroke: Initial clinical results. In: *IEEE International Conference on Rehabilitation Robotics*, Piscataway, pp. 13–16. IEEE (2005)
9. Krebs, H.I., Dipietro, L., Levy-Tzedek, S., et al.: A paradigm shift for rehabilitation robotics. *IEEE Eng. Med. Biol. Mag.* **27**(4), 61–70 (2008)
10. Amirabdollahian, F., Gradwell, E., Loureiro, R., et al.: Effects of the GENTLE/S robot mediated therapy on the outcome of upper limb rehabilitation post-stroke: Analysis of the battle hospital data. In: *8th International Conference on Rehabilitation Robotics*, pp. 55–58 (2003)
11. Harwin, W., Loureiro, R., Amirabdollahian, F., et al.: The GENTLE/S project: a new method of delivering neuro rehabilitation. In: *6th European Conference for the Advancement of Assistive Technology*, Amsterdam, Netherlands, pp. 36–41. IOS Press (2001)
12. Guo, S., Gao, J., Guo, J., Zhang, W., Hu, Y.: Design of the structural optimization for the upper limb rehabilitation robot. In: *2016 IEEE International Conference on Mechatronics and Automation*, pp. 1185–1190 (2016)
13. Jensen, F.V., et al.: The SACSO methodology for troubleshooting complex systems. *AIEDAM* **15**(4), 321–333 (2001)
14. Williams, R.L., Gallina, P., Vadia, J.: Planar translational cable-direct-driven robots. *J. Robot. Syst.* **20**(3), 107–120 (2003)
15. Laribi, M., Carbone, G., Zeghloul, S.: On the optimal design of cable driven parallel robot with a prescribed workspace for upper limb rehabilitation tasks. *J. Bionic Eng.* **16**(3), 503–513 (2019)
16. Chen, Z.Y., Zhang, T.T., Li, Z.H.: Hybrid control scheme consisting of adaptive and optimal controllers for flexible base flexible-joint space manipulator with uncertain parameters. In: *Proceedings of the 9th International Conference on Intelligent Human-Machine Systems and Cybernetics*, pp. 341–345. IEEE, Hangzhou (2017)
17. Zhang, C., Zhang, L.: Kinematics analysis and workspace investigation of a novel 2-DOF parallel manipulator applied in vehicle driving simulator. *Robot. Comput.-Integr. Manuf.* **29**(4), 113–120 (2013)
18. Ferravante, V., Riva, E., Taghavi, M., Braghin, F., Bock, T.: Dynamic analysis of high precision construction cable-driven parallel robots. *Mech. Mach. Theory* **135**, 54–64 (2019)